Can Benzylic Amide [2]Catenane Rings Rotate on Graphite?

Michael S. Deleuze

Contribution from the Instituut voor MateriaalOnderzoek (IMO), Departement SBG, Limburgs Universitair Centrum, Universitaire Campus, B-3590 Diepenbeek, Belgium

Received July 12, 1999

Abstract: The structure and dynamics of two benzylic amide [2]catenanes, bearing phenyl- or thiophenyl-1,3-dicarbonyl groups and physisorbed onto a graphite surface, have been investigated by means of molecular mechanics along with elementary calculations of kinetic rate constants. For the isophthaloyl-based catenane (**1**), a delicate balance between enthalpy and entropy effects is pointed out. On one hand, van der Waals interactions are enhanced in a first series of co-conformations (**A**), including the global energy minimum, which are characterized by a near-parallel deposition and flattening of both macrocycles onto the graphite layer. On the other hand, vibrational entropy is shown to favor a very different mode for physisorption (**B**), with one of the interlocked macrocycles being oriented perpendicular, whereas the other remains parallel to the graphite surface. Both kinds of layout should coexist, the energy difference between the two deposited structures being less than 2 kcal/mol. From the calculated energy barriers and the related rate constants, the **A** mode of adsorption on graphite is shown to strongly impede circumrotational actions. On the other hand, circumrotation of one of the macrocycles is at least partially allowed at rates comparable to those found in a nonpolar solution when catenane **1** adopts a co-conformation of type **B**. The thiophenyl-based catenane (**2**) is found to be already enthalpically driven to a deposition mode of the **B**-type, favoring π-stackings and phenyl−phenyl T-shape complexes within the catenane at the expense of dispersion interactions with the substrate. Although sterically allowed, a full circumrotational process appears in this case to be strongly hindered by physisorption forces, intramolecular interactions, and entropy effects. For catenane **2**, rates of the order of one macrocyclic ring rotation per second are nonetheless reached at moderate temperatures (∼400 K).

1. Introduction

Catenanes (and rotaxanes) are nowadays arousing great interest for their structural and dynamical properties as mechanically interlocked molecular systems.[1] Their most fascinating feature is the rather large freedom for motions of their individual molecular components, which shuttle and rotate relative to each other without breaking covalent bonds, and can be positioned in their location and orientation through the influence of external stimuli.[2,3] One of the most attractive class of compounds with high structural versatility, which was serendipitously discovered[4a] in an attempt to prepare a chemical sensor for CO_2, is that of the benzylic amide catenanes (BAC).[4] In contrast to the co-conformationally[5] locked amide catenanes first identified in 1992 by Hunter[1e] and Vögtle,[1f] the BAC molecules show unambiguous NMR evidence[4] of a full spinning (circumrotation) of the interlocked macrocycles one about another. Their remarkably tolerant synthesis[4b] allows substantial variations in the structure of the precursor, which result in large alterations of the rates of the macrocyclic ring rotation from the microhertz to the kilohertz regime,[6,7] through a calibrated modulation of electronic and steric factors.[8] Variations of the solvent polarity even afford a fine-tuning of the circumrotational motions and of their rate constants.[6] Benzylic amide catenanes are thus ideally suited for the development of nanoscale devices such as molecular switches, shuttles, or information storage systems.[9]

The circumrotation of benzylic amide catenanes is a highly concerted process,[8] which implies considerable molecular rear-

(1) (a) Schill, G. *Catenanes, Rotaxanes and Knots*; Academic Press:. New York, 1971. (b) Sauvage, J.-P. *Acc. Chem. Res.* **1990**, *23*, 319−327. (c) Amabilino, D. B.; Stoddart, J. F. *Chem. Rev.* **1995**, *95*, 2725−2828. (d) Gibson, H. W.; Bheda, M. C.; Engen, P. T. *Prog. Polym. Sci.* **1994**, *19*, 843−945. (e) Hunter, C. A. *J. Am. Chem. Soc.* **1992**, *114*, 5303−5311. (f) Vögtle, F.; Dunnwald, T.; Schmidt, T. *Acc. Chem. Res.* **1996**, *29*, 451−460. (g) Jager, R.; Ahuis, F.; Kray, B.; Vögtle, F.; Liebigs, A. *Recueil* **1997**, 761−766. (h) Gruter, J. G. M.; de Kanter, F. J. J.; Markies, P. R.; Nomoto, T.; Akkerman, O. S.; Bickelhaupt, F. *J. Am. Chem. Soc.* **1993**, *115*, 12179−12180. (i) Fujita, M.; Ibukuro, F.; Hagihara, H.; Ogura, K. *Nature* **1994**, *367*, 720−723. (j) Hamilton, D. G.; Sanders, J. K. M.; Davies, J. E.; Clegg, W.; Teat, S. J. *Chem. Commun.* **1997**, 897−898.

(2) (a) de Silva, A. P.; McCoy, C. P. *Chem. Ind.* (*London*) **1994**, 992. (b) Drexler, K. E. *Annu. Rev. Biophys. Biomol. Struct.* **1994**, *23*, 377. (c) Whitesides, G. M. *Sci. Am.* **1995**, *273* (3), 114. (d) Ward, M. D. *Chem. Ind* (*London*) **1997**, 640.

(3) (a) For catenanes where solvent variations effect circumrotational dynamics and translational isomerism, see: Ashton, P. R.; Ballardini, R.; Balzani, V.; Credi, A.; Gandolfi, M. T.; Menzer, S.; Perez-Garcia, L.; Prodi, L.; Stoddart, J. F.; Venturi, M.; White, A. J. P.; Williams, D. J. *J. Am. Chem. Soc.* **1995**, *117*, 11171−11197. (b) For electrochemically and photochemically driven macrocyclic ring motions in a catenane, see: Livoreil, A.; Sauvage, J.-P.; Armaroli, N.; Balzani, V.; Flamigni, L.; Ventura, B. *J. Am. Chem. Soc.* **1997**, *119*, 12114−12124 and references therein.

(4) (a) Johnston, A. G.; Leigh, D. A.; Pritchard, R. J.; Deegan, M. D. *Angew. Chem., Int. Ed. Engl.* **1995**, *34*, 1209−1212. (b) Johnston, A. G.; Leigh, D. A.; Nehzat, L.; Smart, J. P.; Deegan, M. D. *Angew. Chem., Int. Ed. Engl.* **1995**, *34*, 1212−1216. (c) Leigh, D. A.; Moody, K.; Smart, J. P.; Watson, K. J.; Slawin, A. M.Z. *Angew. Chem., Int. Ed. Engl.* **1996**, *35*, 306−310.

(5) "Co-conformation" refers to the relative positions and orientations of the mechanically interlocked components with respect to each other [Fyfe, M. C. T.; Glink, P. T.; Menzer, S.; Stoddart, J. F.; White, A. J. P.; Williams, D. J. *Angew. Chem., Int. Ed. Engl.* **1997**, *36*, 2068−2070].

(6) Leigh, D. A.; Murphy, A.; Smart, J. P.; Deleuze M. S.; Zerbetto, F. *J. Am. Chem. Soc.* **1998**, *120*, 6458−6467.

(7) For catenanes where structure variations effect circumrotational dynamics, see also: Anelli, P.-L.; Ashton, P. R.; Ballardini, R.; Balzani, V.; Delgado, M.; Gandolfi, M. T.; Goodnow, T. T.; Kaifer, A. E.; Philp. D.; Pietraszkiewicz, M.; Prodi, L.; Reddington, M. V.; Slawin, A. M. Z.; Spencer, N.; Stoddart, J. P.; Vicent, C.; Williams, D. J. *J. Am. Chem. Soc.* **1992**, *114*, 193−218.

(8) Deleuze, M. S.; Leigh, D. A.; Zerbetto, F.; *J. Am. Chem. Soc.* **1999**, *121*, 2364−2379.

10.1021/ja992458a CCC: $19.00
Published on Web 02/01/2000

rangements to overcome many steric and electrostatic constraints, in particular to accommodate the partial disruption of the internal network of hydrogen bonds, π-stacks, phenyl−phenyl T-shape, or herringbone complexes. If the mechanisms[8] by which the macrocycles shuttle and rotate with respect to each other are now well understood for the isolated case[8,10] or in a nonpolar solvent,[6] a detailed investigation of the structure and dynamics of catenanes in thin films or coating surfaces still remains a crucial and mandatory step for the development of practical applications in nanoscale technologies.

Owing to its much too large sampling depth, NMR spectroscopy is of very little use when dealing with adsorbed species or with the top layers of complex materials. The first experimental source of information that comes to mind to unravell thorny physisorbed structures are the scanning tunneling [11] and atomic force microscopies (STM, AFM).[12] However, if atomic motions can be followed in some very ideal cases, results are most often biased by a preconditionning of the samples and great difficulties in extracting information from topographic pictures based, e.g., on complex charge densities. Although well-suited for characterizing adsorbed species, the most common surface-sensitive[13] techniques, based on electron diffraction (e.g. LEED and RHEED), photoelectron spectroscopy,[14] or vibrational analysis (e.g. EELS and HREELS), would be of no use, in view of their characteristic time scales, for investigation of the circumrotational processes occurring in deposited or grafted catenanes. Nowadays, detailed characterization of the dynamics of interlocked molecules on surfaces represents thus certainly one of the very specific problems which can only be tackled on theoretical grounds.

In this contribution I present the very first study of circumrotations in catenanes while they are physisorbed onto a model surface, graphite. The dynamics of catenanes on such an ideal surface represents a very critical topic, in the context of material design. If physisorption on graphite would too strongly hinder circumrotations, the possibility of observing and exploiting these complex and sterically demanding motions should certainly be dismissed for catenanes embedded in more constrained environments (e.g. within thin films or chemisorbed onto a metal surface).

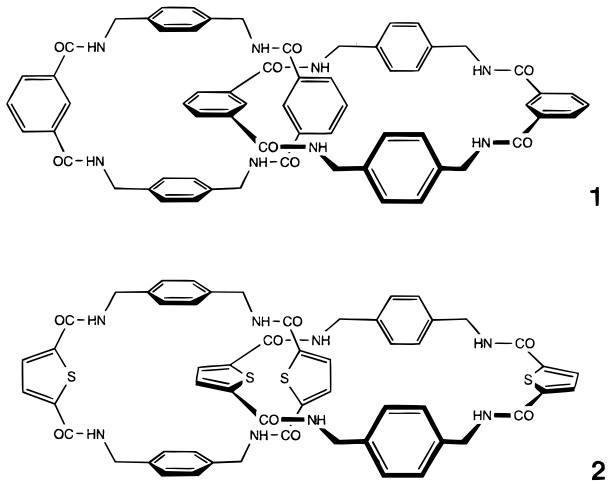

Figure 1. Chemical structure of the selected benzylic amide catenanes: isophthaloyl catenane (**1**) and thiophenyl catenane (**2**).

The goal of the present work is to identify the leading coconformations and energy barriers encountered along the lowest energy paths associated with the circumvolutions of the two homo[2]catenanes displayed in Figure 1, taking into account the constraints (and artifacts) arising from a model finite graphite layer. As a byproduct, the study finds a first application in assessing structural and dynamical conclusions drawn from preliminary STM measurements of monomolecular layers of catenane **1** deposited on highly oriented pyrolitic graphite (HOPG).[15] Owing to the size of the aggregates under consideration and the nature of the investigated processes, calculations have been carried out on the grounds of molecular mechanics,[16] using the MM3 force field.[17−20] The obtained energy barriers are in turn used to characterize the dynamics of the physisorbed catenane by means of elementary treatments of kinetic rate constants, based on the widely used RRKM (Rice, Ramsperger, Kassel, and Marcus) and transition state theories for unimolecular reactions.[21]

2. Theory and Methodology

2.1. The Force Field. Molecular dynamical properties are most commonly characterized in terms of the minima of the potential energy surface (PES), corresponding to locally stable conformations, and of the transition states that connect these minima as first-order saddle-points. For large and versatile systems such as catenanes, the quality of theoretical predictions is highly dependent on the details of the potential. The present work relies on the MM3 potential,[17−20] which represents one of the most complete and reliable force fields for molecular mechanics[16] computations. The approach is particularly well-suited for the treatment of rotational barriers and steric energies in strained (cyclic and cage) structures,[22] of vibrational spectra

(9) (a) Whitesides, G. M.; Mathias, J. P.; Seto, C. T. *Science* **1991**, 254, 1312−1319. (b) Bissell, R. A.; Stoddart, J. F. In *Computations for the Nano-Scale*; NATO ASI Ser. Vol. 240; : Blöchl, P. E., Fisher, A. J.,; Joachim, C., Eds.; Kluwer: Dordrecht, 1993; pp 141−152. (c) Drexler, K. E. *Annu. Rev. Biophys. Biomol. Struct.* **1994**, *23*, 377−405. (d) Anelli, P.-L.; Asakawa, M.; Ashton, P. R.; Bissell, R. A.; Clavier, G.; Górski, R.; Kaifer, A. E.; Langford, S. J.; Mattersteig, G.; Menzer, S.; Philp, D.; Slawin, A. M. Z.; Spencer, N.; Stoddart, J. F.; Tolley, M. S.; Williams, D. J. *Chem. Eur. J.* **1997**, *3*, 1113−1135.

(10) Ballardini, R.; Balzani, V.; Credi, A.; Brown, C. L.; Gillard, R. E.; Montali, M.; Philp, D.; Stoddart, J. F.; Venturi, M.; White, A. J. P.; Williams, B. J.; Williams, D. J. *J. Am. Chem. Soc.* **1997**, *119*, 12503−12513.

(11) STM: (a) Guntherödt, H.-J.; Wiesendanger, R. *Scanning Tunneling Microscopy I*; Springer: Berlin, 1992. (b) Van de Leemput, L. E. C.; Lekkerkerker, H. N. W. *Rev. Prog. Phys.* **1992**, *55*, 1165. (c) Yang, R.; Yang, X. R.; Evans, D. F.; Hendrickson, W. A.; Baker, J. *J. Phys. Chem.* **1990**, *94*, 6123. (d) Rabe, J. P.; Buchholz, S. *Phys. Rev. Lett.* **1991**, 66, 2096.

(12) AFM: (a) Sarid, D. *Scanning Force Microscopy with Applications to Electric, Magnetic and Atomic Forces*; Oxford University Press: New York, 1991. Sarid, D.; Elings, V. *J. Vac. Sci. Technol.* **1991**, *B9*, 431.

(13) (a) Niemantsverdriet, J. W. *Spectroscopy in Catalysis*; VCH Publishers: New York, 1993. (b) Prutton, M. *Introduction to Surface Physics*; Oxford Science Publications, Clarendon Press: Oxford, 1994.

(14) (a) Brundle, C. R.; Baker, A. D. *Electron Spectroscopy: Theory, Techniques and Applications*; Academic Press: London, 1981. For specific applications of photoelectron spectroscopy in conformational assignments, see e.g.: (b) Deleuze, M.; Denis, J. P.; Delhalle, J.; Pickup, B. T. *J. Phys. Chem.* **1993**, *97*, 5115. (c) Deleuze, M.; Delhalle, J.; Pickup, B. T.; Svensson, S. *J. Am. Chem. Soc.* **1994**, *116*, 10715. (d) Duwez, A. S.; Di Paolo, S.; Ghijsens, J.; Riga, J.; Deleuze M.; Delhalle, J. *J. Phys. Chem. B* **1997**, *101*, 884.

(15) Biscarini, F.; Gebauer, W.; Di Domenico, D.; Zamboni, R.; Pascual, J.-I.; Leigh, D. A.; Murphy, A.; Tetard, D. *Synth. Met.* **1999**, *102*, 1466.

(16) Burkert, U.; Allinger, N. L. *Molecular Mechanics*; American Chemical Society: Washington, D.C., 1982.

(17) Allinger, N. L.; Yuh, Y. H.; Lii, J.-H. *J. Am. Chem. Soc.* **1989**, *111*, 8551−8566.

(18) Lii, J.-H.; Allinger, N. L. *J. Am. Chem. Soc.* **1989**, *111*, 8566−8575.

(19) Lii, J.-H.; Allinger, N. L. *J. Am. Chem. Soc.* **1989**, *111*, 8576−8582.

(20) Allinger, N. L.; Lii, J.-H. *J. Comput. Chem.* **1987**, *8*, 1146−1153.

(21) For a review, see: Gilbert, R. G.; Smith, S. C. *Theory of Unimolecular and Recombination Reactions*; Blackwell Scientific Publications: Oxford, 1990.

(22) Patterson, I.; Liljefors, T. *J. Comput. Chem.* **1987**, *8*, 1139−1145.

and related properties (e.g. vibrational entropies),[18] and of through-space interactions between aromatic rings.[20,22] The MM3 results presented here have been obtained using a slightly adapted version of the TINKER package.[23−25] A few additional parameters, required for the treatment of conjugated amides, are available from ref 8. This package includes specific contributions for the out-of-plane deformations of aromatic rings, together with a π-electron self-consistent field (SCF) treatment of the conjugated segments and of their charges, bond lengths, and stretching force constants.

Quite importantly, this force field has already been validated in a systematic exploration[8] of the circumrotational paths of three different benzylic amide catenanes, bearing pyridyl- and as here phenyl- and thiophenyl-1,3-dicarbonyl groups. The MM3 activation energies for the processes were found to nicely reproduce the barriers inferred from temperature-dependent NMR measurements in a nonpolar ($C_2D_2Cl_4$) solution,[6] with discrepancies in the range of 0.5−1 kcal mol^{-1}. One possible reason for the success of MM3 lies in the mechanism of the circumrotation which entails[8] a continuous breaking and reconstruction of the intramolecular network of hydrogen bonds and π-stacks, phenomena for which molecular mechanics is precisely parametrized. Comparable investigations of the spinning of fullerene cages in close-packed clusters have also provided energy barriers in the range of that found in the solid phase.[26] Application of MM3 on large and topologically nontrivial molecules has been further justified by simulations of the inelastic neutron scattering spectra of catenane **1**,[27] and of an inclusion complex of a calix[4]arene.[28] In view of its recent successes, the MM3 force field is assumed to be reliable enough to pursue investigations of the dynamics of catenanes, when they are physisorbed onto a graphite surface.

2.2. Modeling Physisorption. The interactions of the isophthaloyl and thiophenyl benzylic amide [2]catenanes with graphite have been simulated using a model circular graphite layer (Figure 2a) with chemical composition $C_{301}H_{45}$. The radius of this layer is approximately two times larger than the gyration radius of catenanes **1** and **2**, and is thus thought to be extended enough to prevent important edge effects. At first glance, it can also be assumed that the effects of additional layers should be rather limited, since the dispersion (van der Waals) forces prevailing for the physisorption process are very short range (R^{-6}). However, some care is needed, in view of the size of the systems under consideration, the too high mobility and flexibility of isolated graphite sheets, and the presence in the catenane of a number of strongly polar groups (e.g. amide, thiophenyl), which could interact with the substrate through the interplay of longer range polarization (e.g. dipole−induced dipole) forces.[16,25] With the present MM3 scheme, reported[23] as one of the softest molecular mechanics models, such forces are only indirectly and very partially taken into account, via a careful parametrization of *intra*molecular torsional energies.

To evaluate the relevance of calculations based on a single layer, further simulations of the physisorption process of catenane **1** on the graphite bilayer, $(C_{301}H_{45})_2$, displayed in Figure 2b, have been considered. With a MM3-optimized

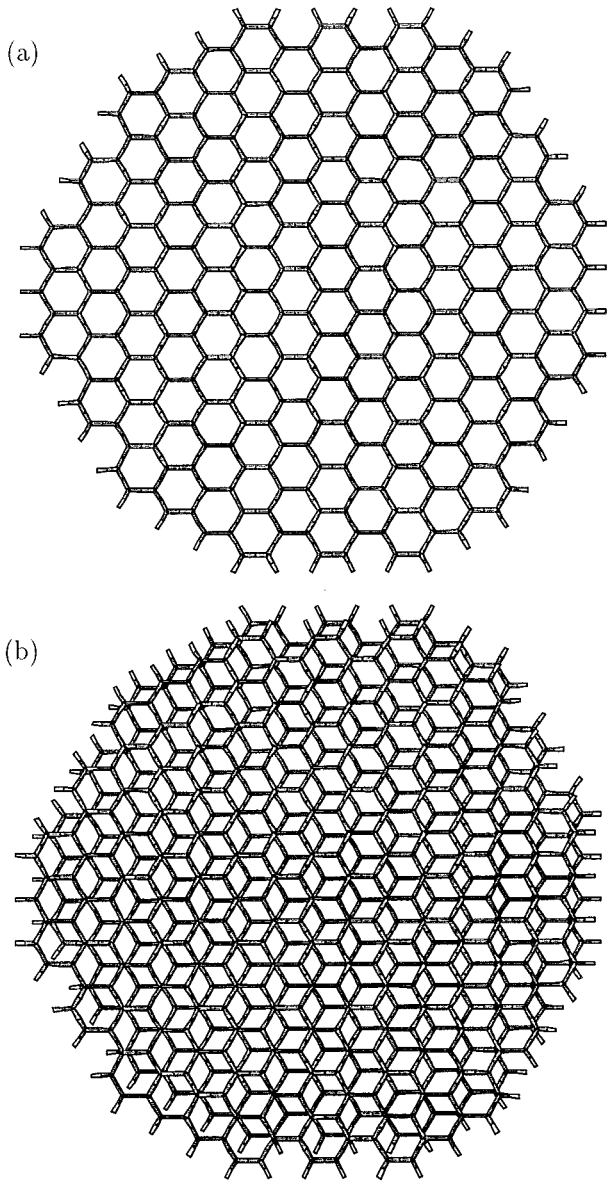

Figure 2. Model graphite layers: (a) $C_{301}H_{45}$ and (b) $(C_{301}H_{45})_2$.

spacing of 3.44 Å between the two layers, and the presence of two different sites in the surface lattice, with and without a carbon neighbor in the second layer, the latter structure closely follows the STM and AFM topographic pictures of graphite.[13a]

The too high flexibility of an isolated graphite monolayer or bilayer in comparison with that of a real graphite surface represents the most important source of error in the modeling. In reality, interactions between many graphite sheets should clearly impede, or at least strongly hinder, the large-amplitude deformations induced by the surface motions of the catenanes to the top layers. Therefore, since this constraint is released, the obtained activation energies for the circumrotational processes will be very likely underestimated values of the barriers that should be encountered on a real graphite surface. Nevertheless, comparison with the isolated case[8] can already be very instrumental in identifying the main factors affecting the structure and dynamics of physisorbed catenanes.

The most demanding part of the MM3 model is the π-electron SCF evaluation[23−25] of the stretching and torsional parameters of the conjugated bonds, in particular within the $C_{301}H_{45}$ graphite layers. To overcome this difficulty and to make possible an extensive investigation of the potential energy surface of its

(23) Ponder, J.; Richards, F. *J. Comput. Chem.* **1987**, *8*, 1016−1024.
(24) Kundrot, C.; Ponder, J.; Richards, F. *J. Comput. Chem.* **1991**, *12*, 402−409.
(25) Dudek, M. J.; Ponder, *J. Comput. Chem.* **1995**, *16*, 791−816.
(26) Deleuze, M. S.; Zerbetto, F. *J. Am. Chem. Soc.* **1999**, *121*, 5281−5296.
(27) Caciuffo, R.; Espoti, A. D.; Deleuze, M.; Leigh, D. A.; Murphy, A.; Paci, B.; Parker S.; Zerbetto, F. *J. Chem. Phys.* **1998**, *109*, 11094.
(28) Paci, B.; Deleuze, M.; Caciuffo, R.; Tomkimson, J.; Ugozzoli, F.; Zerbetto, F. *J. Phys. Chem. A* **1998**, *102*, 6910−6915.

Figure 3. Side views of the reference (a) **A** and (b) **B** physisorbed forms of catenane **1** on $(C_{301}H_{45})_2$ (gray, Mac1; black, Mac2)

complex with the catenane, I used in all calculations the MM3 force constants obtained for the separate $C_{301}H_{45}$ and BAC components, i.e., I assumed that physisorption and intermolecular interactions do not significantly affect the π-electron densities, a fact that was independently verified (see also ref 28). In practice, accounting for the partial release of π-conjugation due to the out-of-plane deformation of the graphite sheets would slightly enhance their flexibility, and thus drift the simulations further apart from the ideal model of a perfectly rigid surface.

A two-step procedure was used to model the physisorption of catenanes **1** and **2** from nonpolar solutions onto the graphite surface. In the first step, many (1200) configurations were generated from random rotations of a reference structure of the catenanes over the whole solid angle, at a large distance (15 Å) from the graphite layer. The selected reference for catenane **1** was optimized[8] by quenching the structure obtained[4a] from X-ray diffraction (XRD) to its closest MM3 minimum. Catenane **2**, on the other hand, has been taken in its global energy minimum (GEM) form, obtained and identified by means of simulated annealing calculations.[8] The reader is referred to ref 8 for details on these structures and for the reasons prevailing in their selection. In a second step, the randomly rotated catenanes were relaxed onto the graphite layer, using a truncated Newton nonlinear optimization procedure.[21] Application of this two-step procedure on catenanes **1** and **2** yielded 250 and 243 different physisorbed structures, respectively, among which are the energy minima presented for catenane **1** in Figures 3 and 4.

2.3. Exploring the Potential Energy Surface. As in a first series of investigations on isolated catenanes,[8] a two-dimensional exploration of the potential energy surface has been performed to account both for shuttling (translations) and pirouetting (i.e. spinning) actions, thus mimicking macrocycle circumrotation in a homocircuit catenane (i.e. of which the two macrocycles are identical). Circumrotational actions are induced by imposing first a series of rigid (uncoupled) rotations to one of the two macrocycles in a selected reference structure. These imply (see Figure 2 in ref 8) a combination of one rotation by an angle θ in the average equatorial plane of the macrocycle and one rotation in a polar plane by an angle ϕ. Iterative series of translations are subsequently applied to the rigidly rotated macrocycle, to identify and release physically unsound (i.e. overcrowded) situations, and to avoid accidental dissociations of the catenane into two unthreaded macrocycles. More details on this rigid rotation & translation (RR&T) protocol can be found elsewhere.[8]

Local distortions neglected in this first step are recovered by the subsequent relaxation to the closest energy minima, using

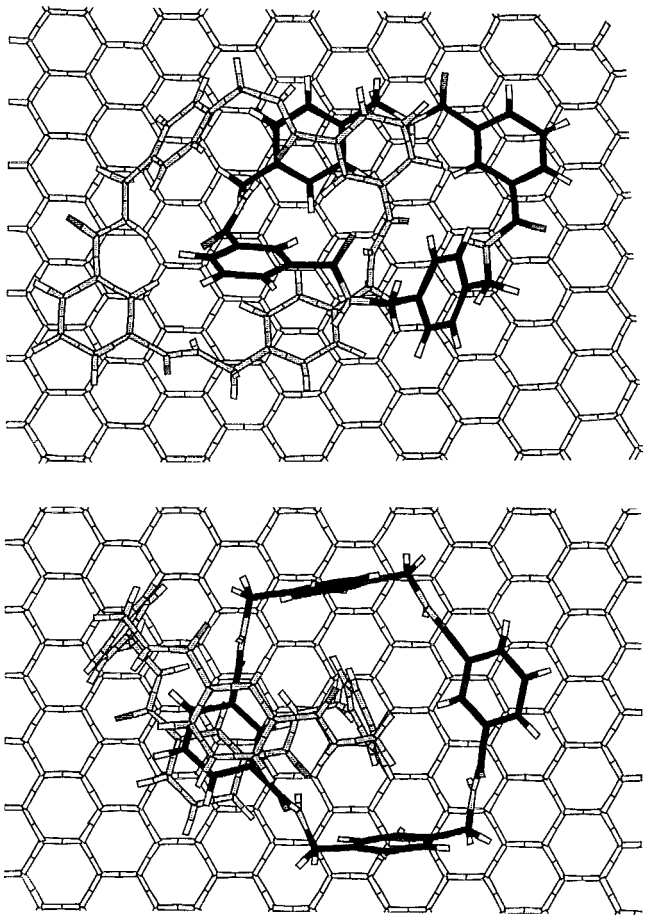

Figure 4. Top views of the reference (a) **A** and (b) **B** physisorbed forms of catenane **1** on $C_{301}H_{45}$ (gray, Mac1; black, Mac2)

the truncated Newton nonlinear optimization procedure.[21] Similarly, relaxations of rigidly rotated structures with the appropriate curvature constraints on the Hessian affords also rather straightforward access to the transition states connecting the main attractors,[8] as first-order saddle points of the potential energy surface. These can be displayed from the infinitesimal mass-weighted atomic displacement vectors associated[8] with the normal vibrational mode with imaginary frequency.

Quite importantly, for convenience and coherence in the following discussion, it is best to assume that once the catenane has been physisorbed and circumrotations have started, one can discriminate between the two macrocycles and therefore assign different labels to them.

2.4. Calculation of Kinetic Rate Constants. Complex and various theoretical schemes have been developed[29] to evaluate the kinetic rate constants associated with unimolecular reactions and transformations, coping with, among others, a strong failure of the adiabatic hypothesis, a significant drainage of the excited states population during the process, strong quantum effects, interferences between multiple decay channels, etc. Benzylic amide catenanes are extremely large compounds, on which such schemes could hardly be applied. In this case, the many vibrational normal modes in the catenanes and the presence of a solid substrate justify the use of the simplest treatment of canonical rate constants, namely, transition state theory (TST):[21]

$$k(T) = \frac{k_B T}{h} \frac{Q^{\ddagger}}{Q} e^{-E_0/k_B T} \quad (1)$$

where Q and $Q^{\ddagger}$ are restricted to the harmonic vibrational partition functions of the minimum and of the transition state, respectively, and with E_0 the activation energy corrected for zero-point vibrational effects.

Despite its simplicity, this very basic approach has already provided semiquantitative insights into the kinetics of ring rotations of benzylic amide catenanes in a nonpolar solvent ($C_2D_2Cl_4$)[8] or fullerene spinning in the solid phase.[26] In particular, ratios between the theoretical MM3/TST[8] and the experimental NMR values[6] were found to range, quite remarkably, from 0.1 to 10. The present MM3/TST study can thus be expected to provide at least a qualitatively reliable description of the structure and dynamics of these catenanes, when physisorbed onto graphite.

3. Results and Discussion

3.1. Isophthaloyl Catenane 1. a. Global and Local Energy Minima. To investigate the circumrotational processes of catenane **1**, a systematic series of 702 rigid rotations and translations ($-180° \le \theta \le 180°$, $-90° \le \phi \le 90°$, with a scanning step of 10°) were applied on a single macrocycle, taking as the reference the GEM form (Figures 3a and 4a) identified via simulated deposition, as described in the Theory and Methodology section. Geometry optimizations of the 143 structures generated via the RR&T algorithm yield 109 additional energy minima, with energies ranging from 0.1 to 30 kcal/mol above the already identified GEM form of catenane **1** on graphite.

Quite importantly, the GEM structure resisted also a test of simulated annealing via molecular dynamics and the Groningen method[30] for coupling to an external bath at 800 °C. This test was performed considering 10 000 dynamic steps of 0.25 fs for thermal equilibration and 80 000 steps of 0.25 fs for the cooling phase, using sigmoidal scaling of temperatures and the velocity Verlet integration method. Except for its more neatly flattened character, the conformation adopted by the physisorbed catenane in the GEM layout is essentially that found in the crystal.[4a] Correspondingly, a C_2 pseudosymmetry prevails for this structure (the isolated XRD-like form is of D_2 symmetry). Like the XRD structure,[4a,8] it is characterized by an internal network of 6 hydrogen bonds, 2 sets of bifurcated bonds and some π-stack interactions linking the two macrocycles to each other.

This first co-conformation (**A**) enhances van der Waals interactions between the graphite substrate and the two macrocycles deposited in a nearly parallel orientation (Figure 3a), both lying in chair form. Inspection of Figures 3a and 4a and the net curvature of the substrate layers (Figure 3a) clearly shows that the physisorption forces affecting catenane **1** are to the largest extent due to parallel (or near parallel) π-stack interactions between graphite and the electron-deprived phenyl rings of two isophthaloyl moieties at the tips of the catenane and two of the four *p*-xylyl units.

Overall, from the atomic coordinates, the **A** co-conformation can be described as a potrusion culminating at ~8.6 Å above the graphite layer, with a basal elliptic surface. The latter can

(29) See e.g.: (a) Pilling, M. J.; Seakins, P. W. *Reaction Kinetics*; Oxford University Press: Oxford, 1995. (b) Baer, T.; Hase, W. L. *Unimolecular Reaction Dynamics, Theory and Experiment*; Oxford University Press: Oxford, 1996. (c) Steinfeld, J. I.; Francisoco, J. S.; Hase, W. L. *Chemical Kinetics and Dynamics*; Prentice Hall: Englewood Cliffs, NJ, 1998. (d) Börjesson, L. E. B.; Nordholm, S.; Anderssojn, L. L. *Chem. Phys. Lett.* **1991**, *186*, 65−72. (e) Truhlar, D. G.; Garett, B. C.; Klippensteing, S. J. *J. Phys. Chem.* **1996**, *100*, 12771−12800 and references therein.

(30) Berendsen, H. J. C.; Postma, J. P. M.; van Gusteren, W. F.; DiNola, A.; Haak, J. R. *J. Chem. Phys.* **1984**, *81*, 3684−3690.

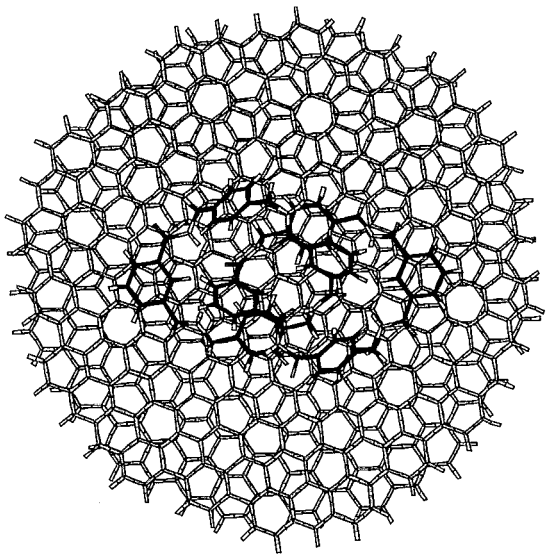

Figure 5. Alteration of the superposition pattern of the two graphite layers after physisorption of catenane **1**.

be roughly characterized by semi-axis of lengths equal to $a = 6.1$ Å and $b = 10.5$ Å. From a comparison of the van der Waals area evaluated for the two components of the BAC**1**−$C_{301}H_{45}$ complex by means of the Connolly's approach[31] with that of the complex itself, an estimate[32] of 258.5 Å^2 is obtained for the area of the contact surface with the graphite substrate. Comparison with the separate energies of the ($C_{301}H_{45}$) monolayer and catenane **1** yields a considerable physisorption heat of $\Delta U_p(0K) = 69.4$ kcal mol^{-1} for the **A** layout. Upon inclusion of zero-point vibrational enthalpies and room-temperature vibrational entropies, $\Delta G_p(298K)$ slightly reduces to 68.5 kcal mol^{-1}, as a result of enhanced constraints on vibrations. When considering the $(C_{301}H_{45})_2$ substrate, these physisorption energies increase to values of $\Delta U_p(0K) = 79.2$ and $\Delta G_p(298K) = 75.6$ kcal mol^{-1}. This increase is mostly an artifact, since it essentially relates to large variations of the interaction forces linking the two model graphite layers with the curvatures induced by the physisorption process, which results in a major but unphysical alteration of their superposition pattern (Figure 5). As sketched in Figure 6, curvatures of the two $C_{301}H_{45}$ layers enable a slightly more favorable relative orientation of the polarized C−H bonds at their edges, leading collectively to a substantial extra stabilization of the complex with the bilayer.

From inspection, the 393 structures generated so far by means of simulated deposition on $C_{301}H_{45}$ or via the RR&T algorithm can be neatly divided into two categories accounting for two drastically different modes for physisorption. A first series clearly displays the same overall pattern as the already discussed **A** form. Within the second conformational series (co-conformation **B**), of which the lowest lying example is displayed in Figures 3b and 4b, only one macrocycle remains parallel to the graphite substrate (more specifically, Mac2), whereas the other one (Mac1) appears to be oriented perpendicular to the surface.

With the **B**-form, the two macrocycles are linked by five hydrogen bonds, of which only two participate to a bifurcated pair. This form lies at $\Delta U(0K) = 6.89$ kcal/mol above the global

(31) (a) Connolly, M. L. *J. Appl. Crystallogr.* **1983**, *16*, 548−558. (b) Connolly, M. L. *J. Am. Chem. Soc.* **1985**, *107*, 118−1124.

(32) The area of the surface contact of a physisorbed form of the catenane (**X** = **A**, **B**, ...) on graphite is obtained as $A_{Contact} = 0.5(A_{Graphite} + A_{Catenane} - A_{Complex})$, with $A_{Graphite}$, $A_{Catenane}$, and $A_{Complex}$ the surface area of the van der Waals exclusion volume of the model graphite monolayer, of the catenane in the **X**-form alone, and of the whole physisorption complex, successively.

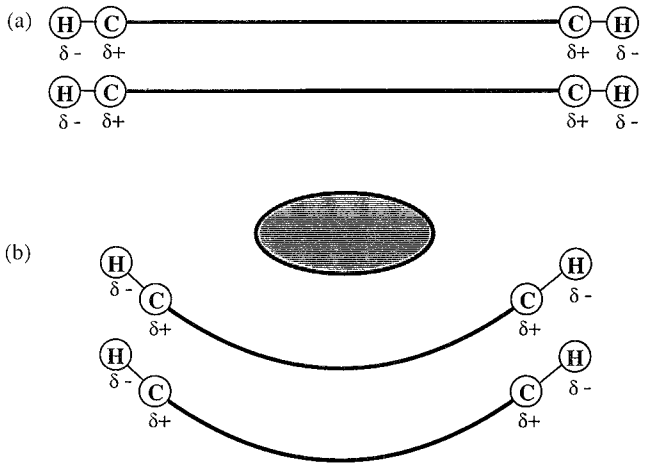

Figure 6. Schematization of edge effects within the model of the $(C_{301}H_{45})_2$ bilayer.

energy minimum, **A**, when considering a single graphite layer as the model substrate. Overall, it can be characterized as a fully asymmetric potrusion, which culminates at 11.2 Å above the graphite surface, and which develops interactions with the substrate over a Connolly−van der Waals contact area of 135.5 Å^2 only. The cohesion forces linking the catenane to the electron-rich graphite surface are mostly limited to π-stacks involving the electron-poorer phenyl unit of two diamide isophthaloyl moieties, and to the intermolecular forces attracting toward graphite the hydrogen atoms of two amide and two *p*-xylyl groups of Mac2. A direct and striking outcome (Figure 3b) of the reduction of the interactions of a catenane lying in the **B**-form with the substrate is the near flatness of the graphite layers, in sharp contrast with the strong curvatures imposed by the **A**-form (Figure 3a). Compared with the latter, the nearly complete and energetically demanding desorption of Mac1 in the **B**-form is susbtantially compensated by the construction of an intricate internal network of π-stack and phenyl−phenyl T-shape complexes, which comprises a triple-decker sandwich involving three isophthaloyl groups, a H-shape complex of three *p*-xylyl units, and a herringbone complex involving one of the *p*-xylyl units in Mac1 and the two isophthaloyl units of Mac2.

Major entropic effects can furthermore be expected for the relative energies of these two forms, owing to a net reduction of vibrational constraints with the second mode for physisorption. From elementary calculations in the harmonic approximation, the energy difference between the two limiting forms reduces indeed further to $\Delta G(298K) = 1.64$ kcal mol^{-1} only, upon inclusion of vibrational zero-point energy [$\Delta(^1/_2\sum_i h\nu_i) = -2.55$ kcal mol^{-1}] and entropy ($\Delta S = +9.05$ cal mol^{-1} K^{-1}). The Gibbs free energy difference increases slightly to $\Delta G(298K) = 2.72$ kcal mol^{-1}, when considering the structures optimized on the graphite bilayer ($\Delta U(0K) = 8.62$ kcal/mol, $\Delta(^1/_2\sum_i h\nu_i) = -2.76$ kcal mol^{-1}, and $\Delta S = +10.55$ cal mol^{-1} K^{-1}). Here again, this variation relates to slight alterations of the superposition pattern of the two graphite layers induced by the evolution of the catenane from the **A**- to the **B**-form, but also to enhanced hindrances to large deformations of the model graphite surface, i.e., the possibility of accommodating at best the interactions with the contact surface of the catenane. In any case, this tiny energy increase, by about 1.1 kcal/mol, gives the magnitude of the errors made on the *relative* energies of different physisorbed co-conformations due to the modeling of the substrate by a monolayer, since it corresponds to one of the largest reductions of the contact surface of the catenane (−48%) that can effectively occur on the graphite surface.

Table 1. Characterization of the Transition States Found for the Threading of a (**I**) *p*-Xylyl and (**II**) Diamide Isophthaloyl Sequence through a Macrocyclic Cavity of Catenane **1**, in Its Two Limiting Physisorption Forms (**A** and **B**) on Graphite

trans. states	obsd passing	$\Delta U^{\ddagger}$ (kcal mol^{-1})	$\Delta H^{\ddagger}$ (kcal mol^{-1})	$\Delta S^{\ddagger}$ (cal mol^{-1} k^{-1})	ω_1 (i cm^{-1})	k(298K) (s^{-1})	k(318K) (s^{-1})	k(338K) (s^{-1})	k(358K) (s^{-1})	k(378K) (s^{-1})	k(398K) (s^{-1})
T1	**I** $-CH_2-$ (**B**)	19.45	19.21	−7.81	39.51	0.106	0.839	5.19	2.62×10^{1}	1.11×10^{2}	4.10×10^{2}
T2	**I** $-CH_2-$ (**B**)	23.29	22.62	−5.83	29.71	4.74×10^{-4}	5.42×10^{-3}	4.68×10^{-2}	3.17×10^{-1}	1.75	8.16
T3	**II** NHCO (**B**)	15.86	14.69	+2.40	55.23	2.71×10^{2}	1.36×10^{3}	5.620×10^{3}	1.99×10^{4}	6.16×10^{4}	1.70×10^{5}
T4	**II** $-C_6H_4-$ (**B**)	16.31	15.44	−8.27	15.86	1.06×10^{2}	5.68×10^{2}	2.50×10^{3}	9.29×10^{3}	3.01×10^{4}	8.68×10^{4}
T5	**II** NHCO (**A**)	26.34	23.53	+0.93	34.21	4.28×10^{-3}	5.78×10^{-2}	5.76×10^{-1}	4.45	2.77×10^{1}	1.44×10^{2}
T6	**II** $-C_6H_4-$ (**A**)	35.32	33.77	−5.36	29.98	5.67×10^{-14}	2.15×10^{-12}	5.30×10^{-11}	9.17×10^{-10}	1.17×10^{-8}	1.17×10^{-7}
T7	**II** $-C_6H_4-$ (**A**)	38.64	36.24	+9.42	15.81	1.92×10^{-14}	9.63×10^{-12}	3.05×10^{-11}	6.58×10^{-10}	1.03×10^{-8}	1.22×10^{-7}

Table 2. Comparison of Results Obtained from Temperature NMR Measurements in $C_2D_2Cl_4$ and from MM3 Calculations on the Isolated Catenane **1** or in Interaction with the Model Graphite Layer[a]

passing		NMR results[b] $C_2D_2Cl_4$ soln	theoretical (MM3) results: isolated catenane[c]	physisorbed catenane (ref A)	physisorbed catenane (ref B)
I	$\Delta U^{\ddagger}$		12.06	*d*	?[e]
$(-C_6H_4-)$	$\Delta G^{\ddagger}$	12.3	12.50	*d*	?[e]
	k	fast	5.40×10^{6}	*d*	?[e]
I	$\Delta U^{\ddagger}$		12.25	*d*	19.5
$(-CH_2-)$	$\Delta G^{\ddagger}$		12.28	*d*	21.54
	k		9.12×10^{3}	*d*	0.733
II	$\Delta U^{\ddagger}$		14.39	35.3	16.31
$(-C_6H_4-)$	$\Delta G^{\ddagger}$	14.5	15.09	33.8	17.90
	k		103	5.90×10^{-12}	106
II	$\Delta U^{\ddagger}$		5.07	26.3	15.86
$(-NHCO-)$	$\Delta G^{\ddagger}$		4.98	23.2	13.97
	k		2.54×10^{9}	1.47×10^{-10}	3170

[a] Theoretical results refer to the lowest transition states identified for the threading of the constituents of the *p*-xylyl (**I**) and diamide isophthaloyl (**II**) segments through the cavity of the spectator macrocycle, taking as reactant state the MM3 form directly derived from the XRD structure in the isolated case, and the **A** and **B** physisorbed co-conformations identified in this work. The $\Delta U^{\ddagger}$ Values are the internal MM3 energy barriers (in kcal mol^{-1}). Room temperature ($T = 298$ K) activation energies ($\Delta G^{\ddagger}$) and TST rate constants (k) are given in kcal mol^{-1} and s^{-1}, respectively. [b] Leigh, D. A.; Murphy, A.; Smart, J. P.; Deleuze, M. S.; Zerbetto, F. *J. Am. Chem. Soc.* **1998**, *120*, 6458−6467. [c] Deleuze, M. S.; Leigh, D. A.; Zerbetto, F. *J. Am. Chem. Soc.* **1999**, *121*, 2364−2379. [d] If transition states are to be found, the corresponding energy barriers certainly largely exceed 35 kcal mol^{-1}. [e] Still open to debate.

Quite remarkably, the identification of two modes for physisorption of catenane **1** on graphite and the small free energy difference between their limiting forms **A** and **B** are qualitatively consistent with a statistical analysis,[15] showing a bimodal distribution of the area of the potrusions seen in ambient STM records of catenane **1** on HOPG. Gaussian fitting of the histogram obtained from these records by F. Biscarini et al.[15] yield effective root-mean-square diameters of 9.5 ± 0.3 and 6.0 ± 0.2 Å, which were said[15] to correlate with the "expected internal" size of the catenane and of a single macrocycle, respectively. However, the corresponding average areas (71 and 28 Å^2) of the potrusions observed in STM are much smaller than the surfaces reported here for the **A**- and **B**-forms. One reason could be the very large freedom for motions of the catenane on the graphite surface (see further), which can be easily swept away by an approaching tip, as seems to be indicated[15] by the lack of correlation between STM images obtained at successive frames.

Since the **B** co-conformation was recovered, after geometry optimization, by applications of the RR&T algorithm onto the **A**-form, these two structures could in principle convert into each other by circumrotations on graphite. In practice, the feasability of the interconversion depends on the energy barriers encountered along the circumrotational paths, an observation that calls for a detailed analysis of the transition states and circumrotational processes in both forms.

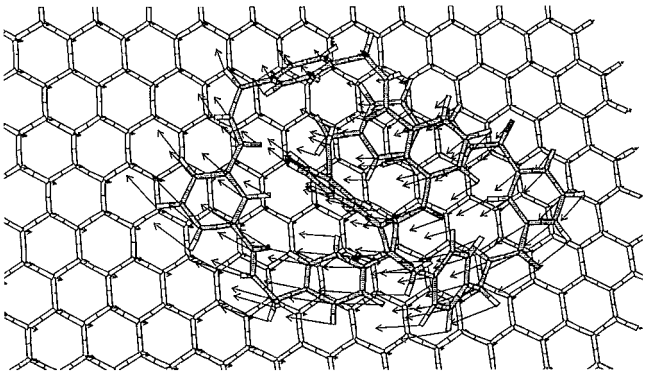

Figure 7. Example of a transition state accounting for a global rotation of catenane **1** on $C_{301}H_{45}$.

b. Transition States. From structural comparisons and a chronological ordering[8] of the identified transition states, the circumrotation path of the isolated catenane **1** (and of its pyridyl and thiophenyl derivatives) could be partitioned[8] into several steps, accounting for the threading of the *p*-xylyl (**I**) or diamide isophthaloyl moieties (**II**) through a macrocyclic cavity. The foremost structural characteristics of the transition states identified along the circumrotational pathway furnished a qualitative and mechanistic interpretation[8] of the large variation of the dynamical behavior observed from one catenane to the other. When considering catenane **1** in its isolated form, the passing *p*-xylyl fragment forms a phenyl−phenyl T-shaped complex with one of the isophthaloyl groups of the threaded macrocycle, an arrangement which led us[8] to characterize the involved transition states as "perpendicular". These states correspond to energy barriers of $\Delta G^{\ddagger}(298\text{ K}) = 12-13$ kcal mol^{-1} and room-temperature TST rate constants of about 3000−9000 s^{-1}, respectively. In the isolated case, the rate-determining step for circumrotation is the passing of the isophthaloyl unit, which in the most favorable case requires an activation energy of $\Delta G^{\ddagger}(298\text{ K}) = 15.1$ kcal mol^{-1}, leading to a kinetic constant of $\sim$100 s^{-1} at room temperature. In the associated transition state, the passing phenyl ring is stacked between two *p*-xylyl units in a triple-decker sandwich of aromatic rings, an arrangement that led us[8] to define this mode for threading as "parallel".

Only fragmentary information could be obtained on the circumrotational paths of the physisorbed catenane (Table 1), in sharp contrast with the isolated case,[8] for which it has been possible to identify a respectable number of transition states for the whole process (see e.g. Table 2). On the other hand, application of the same RR&T + relaxation procedure led to the identification of many smooth transition states of the type of Figure 7, with imaginary frequencies as small as 1 to 10 cm^{-1}, requiring activation energies as low as 1 (!) to 8 kcal mol^{-1}, and accounting for a global displacement and/or rotation

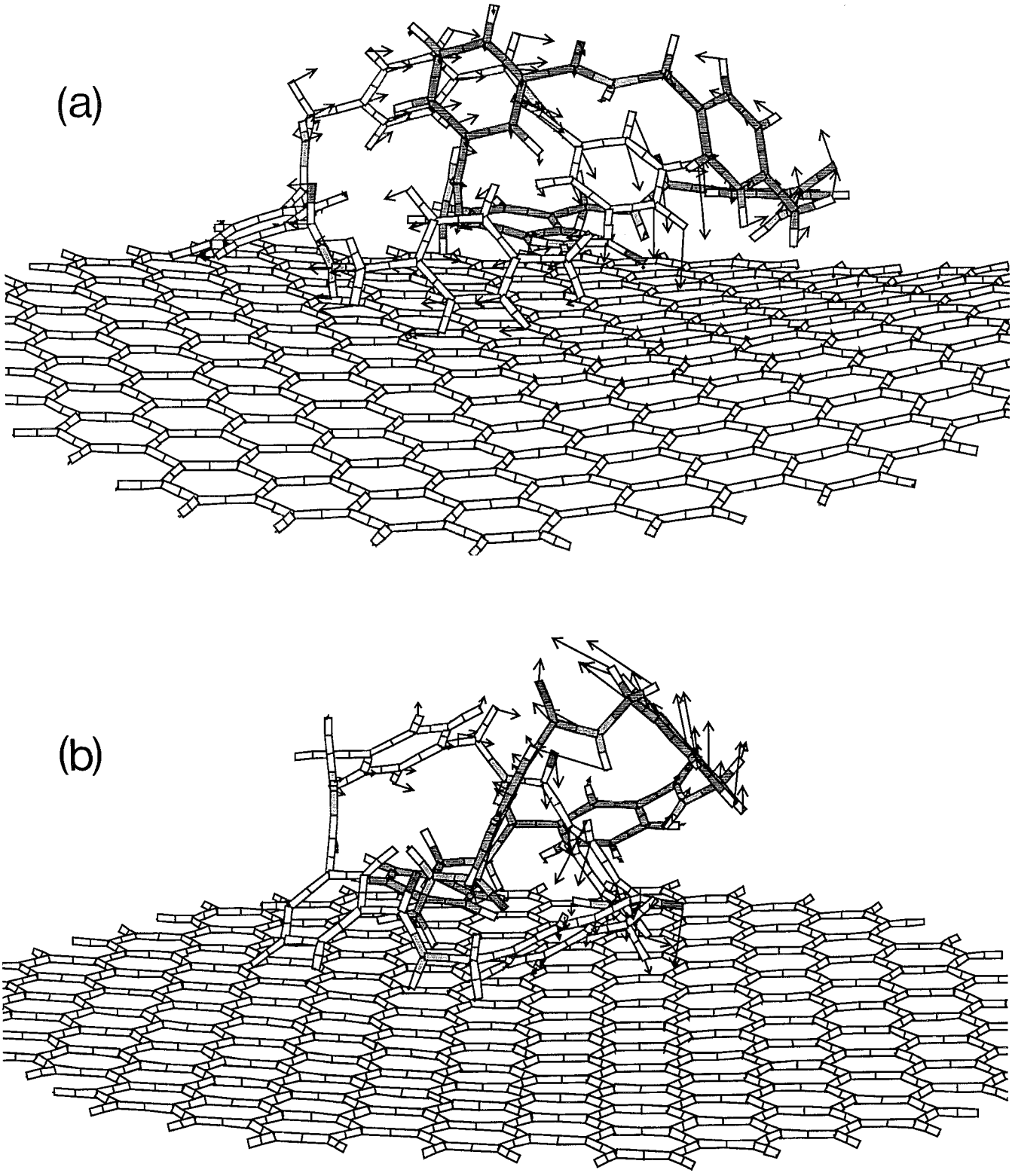

Figure 8. Transition states identified along the circumrotational paths of catenane **1** by application of the RR&T algorithm on Mac1 in its **A**-form of physisorption on $C_{301}H_{45}$: (a) phenyl (**II**) station and (b) amide station (pale gray, Mac1; deep gray, Mac2).

of the catenane on graphite. Despite huge adsorption heats, the MM3 potential energy surface confirms thus the suggestion that benzylic amide catenanes can rotate or translate nearly freely on highly oriented pyrolitic graphite.

The presence of such states complicates the identification of the barriers pertaining to circumrotational processes of a physisorbed catenane. As a result, only a few relevant transition states could be identified (Table 1), to account for the threading of the methylenic and phenyl groups of a *p*-xylyl segment (**I**), and of the amide and phenyl units of an isophthaloyl moiety (**II**), through a macrocyclic cavity. The rather limited success of this search is already an indication of the severe steric and cohesive demands arising from the surface during the circumrotation.

Quite obviously, the most severe demands occur when catenane **1** adopts the physisorption mode of type **A**. In this case, only transition states associated with a diamide isophthaloyl sequence in a rotating macrocycle (Mac1) could be

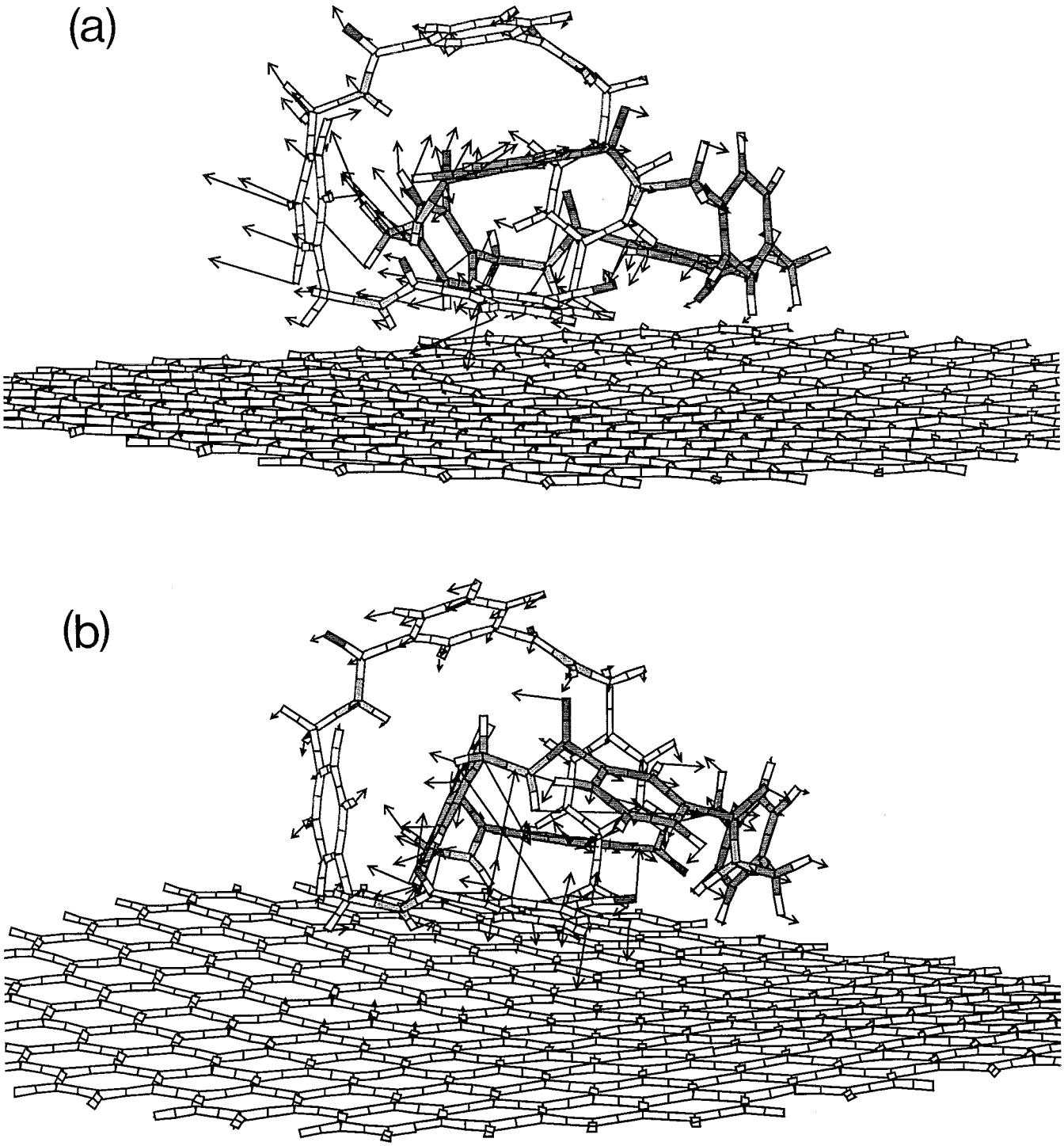

Figure 9. Transition states identified along the circumrotational paths of catenane **1** by application of the RR&T algorithm on Mac1 in its **B**-form of physisorption on $C_{301}H_{45}$: (a) phenyl (**II**) station and (b) $-CH_2-$ station (pale gray, Mac1; deep gray, Mac2).

identified (Figures 8). Clearly, the most striking structural features of the phenyl (**II**) step (Figure 8a) are reminiscent of those found in the isolated case,[8] in view of a near-parallel stacking of the passing phenyl ring between the two *p*-xylyl units of Mac2. As in the isolated case, these actions imply the breaking of one of the hydrogen bonds linking the two macrocyles. In addition, the identified amide station implies also a nearly complete desorption of the "spectator" macrocycle, Mac2, from the $C_{301}H_{45}$ layer. Because of the very strong steric and cohesive interactions imposed by the nearby surface, these transition states are quite naturally characterized (Tables 1 and 2) by much higher activation energies (at least 33.4 kcal mol^{-1}) than those calculated for an isolated molecule or measured in solution. These, in turn, yield rate constants that practically vanish (i.e. rate constants as small as 10^{-14} s^{-1}). Clearly, by extrapolation of the foremost structural features of the transition states displayed in Figures 8, the "perpendicular" mode found[8] for the passing of the *p*-xylyl unit in solution would require even higher energies, since it is more sterically demanding and would thus enhance the detachment of Mac2 from the $C_{301}H_{45}$ layer. Despite the very limited content of the information obtained, the structural and energetic characteristics of the identifed transition states are thus enlightening and conclusive enough to exclude any possibility of circumrotation with decent

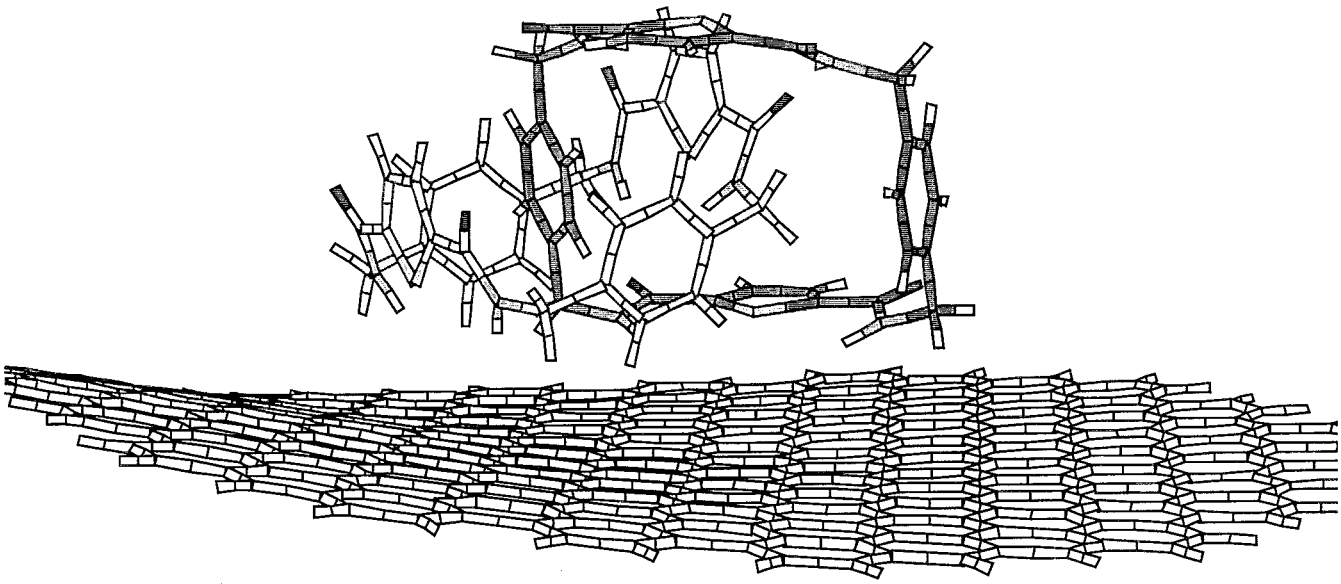

Figure 10. Global energy minimum form of catenane **2** on $C_{301}H_{45}$ (pale gray, Mac1; deep gray, Mac2)

rates on graphite, when the catenane lies in an **A**-type physisorption mode.

As with reference **A**, the circumrotation of the macrocycle lying perpendicularly to the surface (*defined as Mac1*) in the **B**-form would also imply partial but very substantial detachments of the other macrocycle, which in this co-conformation appears to be nearly completely physisorbed on graphite. Since these rearrangements very certainly require huge activation energies, it has been decided to focus on the circumrotational processes associated with the macrocycle oriented parallel to the graphite layer (i.e. *Mac2*), when considering the physisoption mode of type **B**. The results obtained for reference **B** indicate that, in this case, circumrotation of Mac2 is at least partially allowed, since several transition states of relatively low energy could be identified (Table 1) for the threading of a diamide isophthaloyl sequence of Mac2 through the cavity of Mac1. As in the isolated case, the rate-determining step associated with the $-NH-CO-C_6H_4-CO-NH-$ sequence is determined by the phenyl (**II**) station (Figure 9a). Here again, the structural features associated with these transition states, in particular the triple-decker sandwich involving the phenyl rings of two *p*-xylyl units and of the passing isophthaloyl segment, imply that this mode for threading can be referred to as "parallel". Taking reference **B** as the reactant state, this transition state corresponds to an energy barrier of $\Delta G^{\ddagger}(298K)=17.9$ kcal mol^{-1} only (Table 2). Interestingly, the slight increase in the activation energies due to the graphite surface is compensated by strong preexponential factor effects, reflecting strong variations of vibrational entropy, and yielding for that passing a rate constant comparable (Table 2) to that found for the rate-determining step in a nonpolar solution,[1,8] of the order of 100 s^{-1}.

Here also, the "perpendicular" mode for the threading of a *p*-xylyl unit of Mac2 inside the cavity of Mac1 is strongly disfavored, because of the steric demand of the central phenyl−phenyl T-shaped complex, and as it would imply a substantial desorption of the rotating macrocycle from the graphite. Quite remarkably, two transition states, with the characterisitics of a "parallel" passing, could be identified (Table 1) for one of the $-CH_2-$ stations (see e.g. Figure 9b) in the *p*-xylyl sequence. Certainly because of the steric constraints arising from the surface these states incorporate substantial local distortions such as pedallings of amides and twistings of aromatic groups, and yield correspondingly (Table 2) significantly larger energy barriers [$\Delta G^{\ddagger}(298K)=22-24$ kcal mol^{-1}] and smaller rate constants. At this stage, it is still not clear yet whether a full circumrotation process on graphite would be feasible or not with a significant rate, since no transition state could be identified for the phenyl (**I**) station.

3.2. Thiophenyl Catenane 2. a. Global and Local Energy Minima. As for catenane **1**, another systematic series of 702 rigid ring rotations and translations (RR&T) has been applied to the most stable structure identified among the 243 physisorbed structures obtained by modeling the deposition process (see Theory and Methodology section), using a scanning step of 10° to explore the circumrotational path of catenane **2** over the whole solid angle ($-180° \le \theta \le 180°$, $-90° \le \phi \le 90°$). Geometry optimizations of the 416 structures generated in this second RR&T step provide us with 218 additional energy minima, among which is the structure displayed in Figure 10. The latter has been identified as the global energy minimum form of catenane **2** on graphite on the grounds of simulated annealing calculations, considering the same procedure as that used for catenane **1**.

This form resembles, to some extent, the **B** physisorption form of catenane **1** (Figures 3b and 4b), since one of the macrocycles (defined as Mac1) lies nearly parallel to the $C_{301}H_{45}$ model layer, whereas the other (Mac2) potrudes obliquely from the graphite surface, up to a relative height of about 10.1 Å. Here also, its constituents adopt a disposition pattern that clearly favors the development of stabilizing interactions between the two macrocycles, at the expense of the weaker dispersion forces with graphite. One should in particular notice in Figure 10 the orientation and exclusion from the cavity of Mac2 of the two thiophenyl rings of Mac1, which obviously helps to preserve internal N−H···S bridges as well as van der Waals interactions between sulfur atoms and the substrate. The area of the contact surface of the GEM form of catenane **2** on graphite is thus particularly limited, 116 Å^2 only. Quite naturally, therefore, the deposition process of catenane **2** on $C_{301}H_{45}$ leads, in comparison with that found for catenane **1**, to slightly more modest physisorption energies [$\Delta U_p(0K) = 62.7$ kcal mol^{-1} and $\Delta G_p(298K) = 60.9$ kcal mol^{-1}, when taking into account harmonic vibrational entropies and zero-point energies].

Table 3. Characterization of the Transition States Found for the Threading of a (**I**) *p*-Xylyl and (**II**) Thiophenyl-1,3-diamide Sequence through a Macrocyclic Cavity of the Thiophenyl-Based Catenane **2** Physisorbed on Graphite

trans. states	obsd passing	$\Delta U^{\ddagger}$ (kcal mol^{-1})	$\Delta H^{\ddagger}$ (kcal mol^{-1})	$\Delta S^{\ddagger}$ (cal mol^{-1} k^{-1})	ω_1 (i cm^{-1})	k(298K) (s^{-1})	k(318K) (s^{-1})	k(338K) (s^{-1})	k(358K) (s^{-1})	k(378K) (s^{-1})	k(398K) (s^{-1})
T1	**I** C_6H_4 (**2**)	15.21	15.84	−14.58	37.88	2.93×10^{-2}	1.51×10^{-1}	6.40×10^{-1}	2.31	7.25	2.03×10^{1}
T2	**I** C_6H_4 (**2**)	15.45	15.96	−14.47	37.96	2.65×10^{-2}	1.39×10^{-1}	5.95×10^{-1}	2.17	6.89	1.95×10^{1}
T3	**I** C_6H_4 (**2**)	20.68	20.54	−5.37	27.63	1.16×10^{-3}	1.05×10^{-2}	7.33×10^{-2}	4.12×10^{-1}	1.93	7.76
T4	**I** CH_2 (**2**)[a]	20.88	21.38	−17.67	12.08	2.85×10^{-5}	2.72×10^{-4}	1.99×10^{-3}	1.17×10^{-2}	5.65×10^{-2}	2.34×10^{-1}
T5	**II** C_4SH_2 (**2**)	28.74	28.38	+9.33	12.80	8.28×10^{-5}	7.35×10^{-4}	4.89×10^{-3}	2.63×10^{-2}	1.19×10^{-1}	5.58×10^{-1}
T6	**II** NHCO (**1**)	3.45	3.41	−11.03	37.00	1.04×10^{10}	1.52×10^{10}	2.13×10^{10}	2.88×10^{10}	3.77×10^{10}	4.80×10^{10}
T7	**II** NHCO (**1**)	4.02	4.10	−3.27	35.55	1.84×10^{9}	2.90×10^{9}	4.33×10^{9}	6.18×10^{9}	8.49×10^{9}	1.13×10^{10}
T8	**II** NHCO (**2**)	18.47	18.30	−9.40	48.24	2.70×10^{-1}	1.96	1.12×10^{1}	5.31×10^{1}	2.13×10^{2}	7.41×10^{2}
T9	**II** NHCO (**1**)	19.04	19.49	−9.64	48.23	4.96×10^{-4}	3.94×10^{-3}	2.44×10^{-2}	1.24×10^{-1}	5.28×10^{-1}	1.95
T10	**II** NHCO (**2**)	22.33	21.17	−5.21	51.24	9.12×10^{-3}	9.12×10^{-2}	7.03×10^{-1}	4.31	2.19×10^{1}	9.44×10^{1}
T11	**II** NHCO (**1**)	31.98	32.35	−11.73	31.60	5.72×10^{-14}	1.76×10^{-12}	3.63×10^{-11}	5.32×10^{-10}	5.88×10^{-9}	5.10×10^{-8}

[a] Enables also **I** C_6H_6 (**1**) in the perpendicular mode.

The foremost structural features of the GEM form of catenane **2** on graphite are a triple-decker sandwich of one *p*-xylyl unit of Mac2 by two thiophenyl 1,3-diamide units of Mac1, and a herringbone complex of the phenyl core of the same *p*-xylyl unit with the two phenyl rings of Mac1. In addition, this co-conformation of catenane **2** is characterized by an internal network of 8 N−H···S bridges, and 2 hydrogen bonds. It differs markedly from the GEM form of the isolated catenane,[8] based on a quadruple-decker sandwich of thiophenyl rings, and an internal network of 4 inter-ring hydrogen bonds and 6 intra-ring N−H···S bridges. These observations entail thus major structural rearrangements in the presence of the graphite surface, such as a rotation of one of the macrocycle (Mac2) by about 90° in its equatorial plane and 45° in the polar direction, and the reversal of two exo N−H bonds from a transoid to a more favorable cisoid conformation.

With the GEM form displayed in Figure 10, the prevailing physisorption forces for Mac2 arise essentially from a π-stack interaction between the graphite substrate and a 1,3-thiophenyl diamide sequence. On the other hand, interactions of Mac1 with graphite are essentially limited to the sulfur atom of one thiophenyl ring, and a number (8) of hydrogen atoms belonging to two amide and two π-xylyl groups. This, together with the experience gained with catenane **1**, led me to initiate the exploration of the circumrotational paths of catenane **2** by generating from this form a third set of 403 rigidly rotated structures, obtained again using a RR&T chart of 702 points and a scanning step of 10° over the whole solid angle pertaining to the equatorial and polar rotations (θ and ϕ) of the macrocycle lying parallel to the graphite substrate, i.e., Mac1.

b. Transition States. Besides a number of transition states accounting for global displacements (rotation and translation) on the graphite surface at very low energetic costs ($\Delta U^{\ddagger} > 1$ kcal mol^{-1}), 11 energy barriers corresponding to circumrotational events in catenane **2** could be identified (Table 3), considering only one reference, the GEM form. In contrast with catenane **1**, at least one transition state could be found (Table 3, Figures 11a,b and 12a,b) to account for a circumrotational action on graphite for each of the constitutive groups of catenane **2**, namely a C_6H_4 and CH_2 unit in a *p*-xylyl segment (**I**), and a C_4SH_2 and CO−NH unit of a 1,3-thiophenyl diamide sequence (**II**). Compared with catenane **1**, the calculated internal energy barriers are also overall lower.

In comparison with the more limited success of comparable searches for catenane **1**, these observations indicate that circumrotations are at first glance sterically easier in this case, owing to the widening of the macrocyclic cavities with the replacement of four six-membered phenyl groups by smaller five-membered thiophenyl rings. This corroborates also results

Table 4. Comparison of Results Obtained from Temperature NMR Measurements in $C_2D_2Cl_4$ and from MM3 Calculations on the Isolated Catenane **2**, or in Interaction with the Model Graphite Layer[a]

			theoretical (MM3) results	
passing		NMR results[b] $C_2D_2Cl_4$ solution	isolated catenane[c]	physisorbed catenane
I	$\Delta U^{\ddagger}$		11.95	15.21
(−C_6H_4−)	$\Delta G^{\ddagger}$		10.52	20.18
	k		1.60×10^{5}	2.93×10^{-2}
I	$\Delta U^{\ddagger}$		14.38	20.88
(−CH_2−)	$\Delta G^{\ddagger}$	11.6	11.90	26.64
	k	9.6×10^{3}	1.24×10^{4}	2.85×10^{-5}
II	$\Delta U^{\ddagger}$		5.42	28.74
(−C_4SH_2−)	$\Delta G^{\ddagger}$	*d*	4.24	25.96
	k	fast	7.80×10^{9}	8.28×10^{-5}
II	$\Delta U^{\ddagger}$		8.26	3.45
(−NHCO−)	$\Delta G^{\ddagger}$	*d*	5.47	6.74
	k	fast	6.44×10^{8}	1.04×10^{10}

[a] Theoretical results refer to the lowest transition states identified for the threading of the constituents of the *p*-xylyl (**I**) and thiophenyl-1,3-diamides (**II**) segments through the cavity of the spectator macrocycle. The $\Delta U^{\ddagger}$ values are the internal MM3 energy barriers (in kcal mol^{-1}). Room temperature ($T = 298$ K) activation energies ($\Delta G^{\ddagger}$) and TST rate constants (k) are given in kcal mol^{-1} and s^{-1}, respectively. [b] Leigh, D. A.; Murphy, A.; Smart, J. P.; Deleuze, M. S.; Zerbetto, F. *J. Am. Chem. Soc.* **1998**, *120*, 6458−6467. [c] Deleuze, M. S.; Leigh, D. A.; Zerbetto, F. *J. Am. Chem. Soc.* **1999**, *121*, 2364−2379. [d] Too low to measure experimentally.

obtained from the MM3 potential energy surface of this catenane in the vacuum,[8] or from NMR measurements[6] in a nonpolar solution. The latter (Table 4) provided only one significant energy barrier of 11.6 kcal mol^{-1} along the circumrotational paths. The MM3/TST results showed that this barrier can be assigned to the threading through a macrocyclic cavity of a *p*-xylyl segment, the phenyl core of which is facing the sulfur lone pairs of a perpendicularly oriented thiophenyl ring in the spectator macrocycle.[8] Threading of 1,3-thiophenyl diamide sequences was found to require very little energy (Table 4), since the vacuum reference structure enables an easy access to nearby "parallel" transition states which preserve its internal network of hydrogen bonds and helicoidal π-stacks of thiophenyl rings.[8] Since deposition on graphite strongly perturbs the architecture of catenane **2**, one may thus expect already significant differences with physisorbed species.

Quite remarkably, it appears that the two macrocycles can exchange their role when compared to the rotational action imposed on Mac1 with the RR&T algorithm, since in a number of cases (Table 3) the pirouetting action ultimately observed can be thought of as due to Mac2 (see e.g. Figure 11a). The crossing point for this swapping is the "parallel" phenyl (**I**)

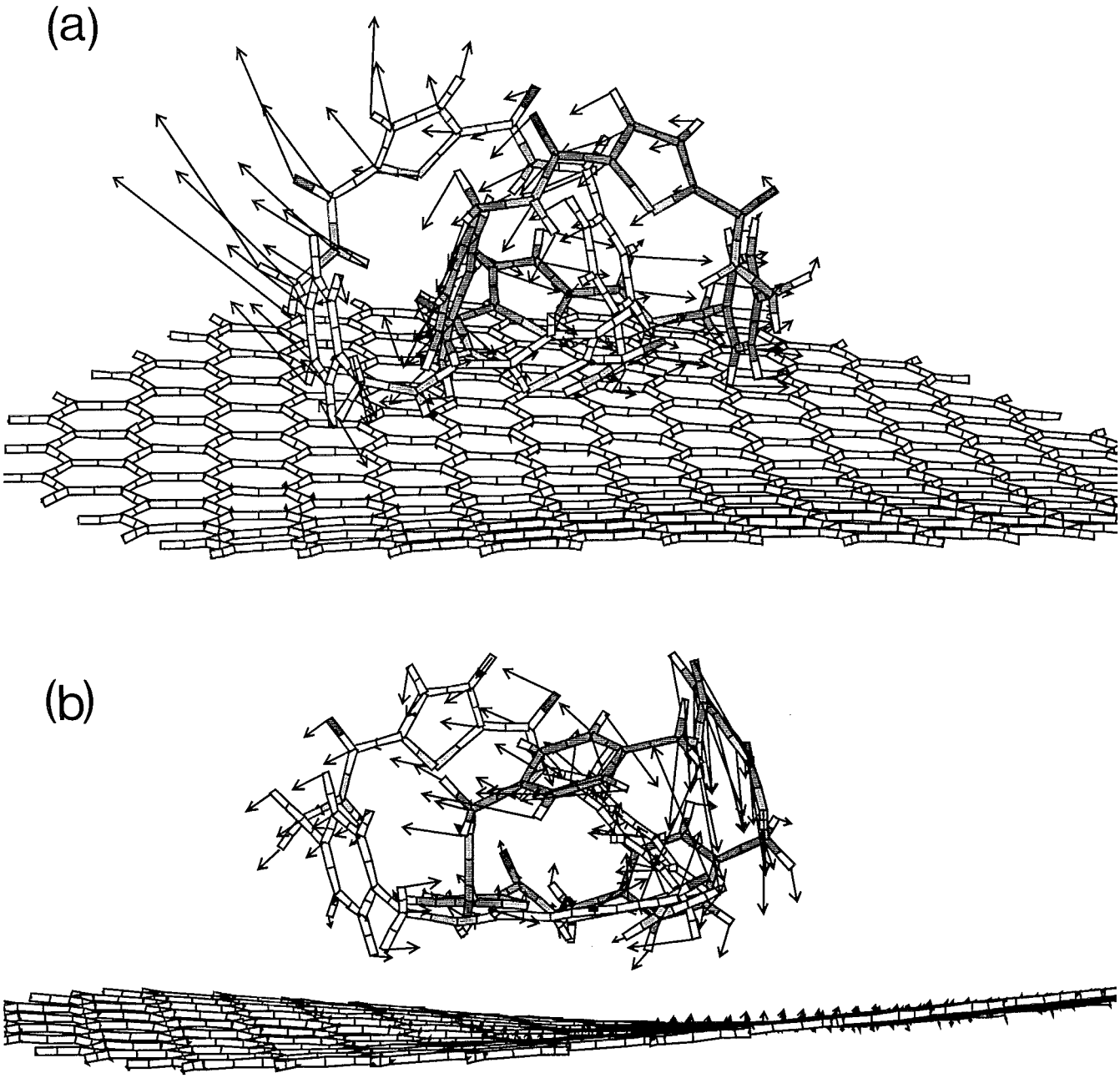

Figure 11. Transition states identified along the circumrotational paths of catenane **2** by application of the RR&T algorithm on Mac1 in its GEM form of physisorption on $C_{301}H_{45}$: (a) phenyl (**I**) station in Mac2 and (b) phenyl (**I**) station in Mac1 combined with a $-CH_2-$ station in Mac2 (pale gray, Mac1; deep gray, Mac2).

station of Figure 11a, of which the foremost structural features are the overall equivalence of the two macrocycles within a supramolecular architecture of pseudosymmetry C_2, and a central quadruple-decker sandwich containing the four phenyl rings of the catenane. This transition state is also characterized by one fewer N−H···S bridge than in the reference GEM structure. The area (112 Å^2) of the surface contact with the graphite surface in this transition state is practically identical with that of the reference GEM form. The first direct result of a very favorable balance of steric, electrostatic, and dispersion interactions is a quite acceptable MM3 energy barrier of $\Delta U^{\ddagger} = 15.2$ kcal mol^{-1}, i.e., only 3.3 kcal mol^{-1}(Table 4) above the energy required for the same passing in the vacuum. Quite unfortunately, however, the rather compact and strained nature of this transition state results in a substantial decrease of vibrational entropy (Table 3) compared to the reference reactant state, which yields ultimately (Table 4) a rather important activation energy [$\Delta G^{\ddagger}$(298K) = 20.2 kcal mol^{-1}]. Physisorption on graphite thus seriously affects the kinetics of the phenyl (**I**) station (a TST rate constant of 0.03 s^{-1} only is obtained at room temperature), without forbidding it completely.

Although substantially higher in energy [$\Delta U^{\ddagger} = 20.9$ kcal mol^{-1}], the rather closely related first-order transition state displayed in Figure 11b is particularly attractive since it affords a double circumrotational action, implying clockwise−anticlockwise rotations of the two macrocycles, and thus confirming the suggestion[8] that Mac1 and Mac2 can rather easily swap their role in a catenane with reduced steric demands. This state accounts for the threading of the phenyl core of a *p*-xylyl unit of Mac1 through a herringbone complex involving the two phenyl rings of Mac2, and for the passing of a methylenic unit of Mac2 through the cavity of Mac1. Since the following phenyl

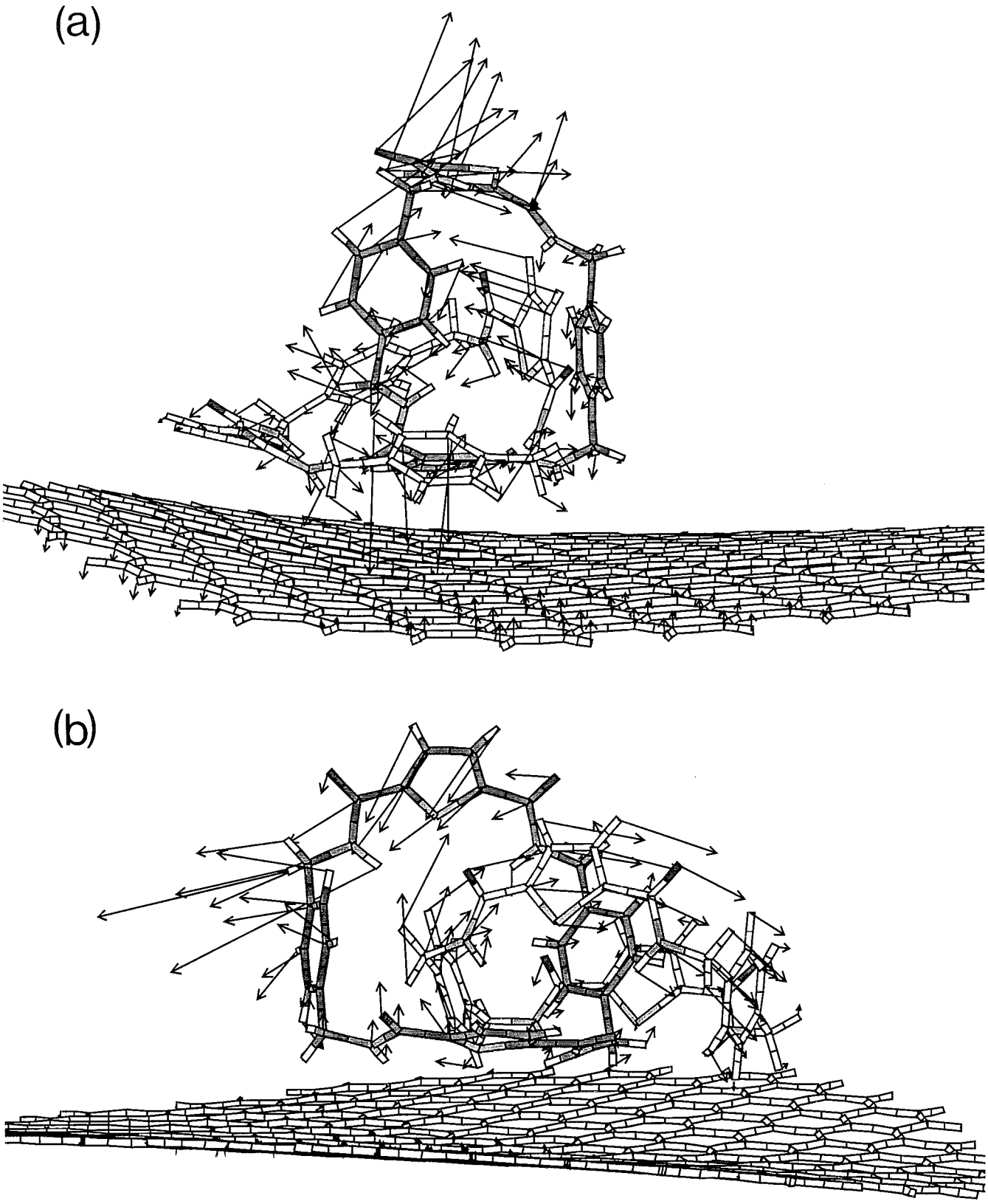

Figure 12. Transition states identified along the circumrotational paths of catenane **2** by application of the RR&T algorithm on Mac1 in its GEM form of physisorption on $C_{301}H_{45}$: (a) thiophenyl station in Mac1 and (b) amide station in Mac1 (pale gray, Mac1; deep gray, Mac2)

ring is itself embedded in a π-stack with a thiophenyl ring of Mac1, the $-CH_2-$ station of Mac2 is consistent with the modalities of a "parallel" mode for passing, whereas the phenyl (**I**) station identified in this case for Mac1 can be referred to as "perpendicular". The highly strained nature of this transition state yields also a very unfavorable decrease of vibrational entropy (Table 3) leading at room temperature to (Table 4) a large energy barrier of $\Delta G^{\ddagger}(298\text{K}) = 26.6$ kcal mol^{-1} and a deceptively too low rate constant of 3×10^{-5} s^{-1}.

Also highly energetically demanding [$\Delta U^{\ddagger} = 28.7$ kcal mol^{-1}] is the only transition state (Table 3) clearly identified (Figure 12a) as a thiophenyl station of Mac1. In view of the

overall perpendicular orientation of Mac2 with respect to the graphite layer, this structure has some similarities with the GEM physisorbed form (Figure 10) of catenane **2**. However, it differs markedly from the reference reactant state by its internal network of intermolecular forces. It is first characterized by one fewer hydrogen bond, and the desorption and reversal of an endo N−H bond of Mac2 from a cisoid to transoid conformation, thereby reducing by one the number of N−H···S bridges in the transition state. This amide rotamerization precedes a shuttling of Mac2 along the thread of Mac1 from the phenyl core of the *p*-xylyl sequence to this nearby reversed and desorbed amide group. This in turn results in a considerable release of the internal network of π-stacking and phenyl−phenyl T-shape interactions, which is found to reduce to a single π-stack of one phenyl ring of Mac2 with the passing thiophenyl ring of Mac1. Such an important release of forces with a strong electrostatic component explains both the high internal MM3 energy barrier $\Delta U^{\ddagger}$ and the positive sign of the activation entropy $\Delta S^{\ddagger}$ associated with this state (Table 3). It is partially compensated by a substantial increase by about 20 Å^2 of the area of the contact van der Waals surface between the catenane and the $C_{301}H_{45}$ model layer, which corresponds mostly (compare Figures 12a and 10) to a flattening on graphite of a large fragment, $-HN-CO-C_4SH_2-CO-NH-CH_2-C_6H_4-CH_2-$, of Mac1. Although the possibility of finding transition states at lower energies can never be completely excluded, these very complex rearrangements indicate that physisorption of catenane **2** on graphite tends to dramatically increase the steric and electrostatic demand arising from the thiophenyl station, in comparison with the results obtained for an isolated form (Table 4). Their ultimate outcome is a large energy barrier of $\Delta G^{\ddagger}(298\text{K}) = 26.0$ kcal mol^{-1} and a rather disappointing rate constant of 3×10^{-5} s^{-1} at room temperature (Table 4). Notice, however, that a rate constant of 0.6 s^{-1} can be reached at 125 °C (Table 3).

On the other hand, threading amide units through macrocyclic cavities of the physisorbed catenane does not require significantly larger activation energies than in the vacuum (Table 4), when considering the lowest identified transition states identified for this event (e.g. Figure 12b). As for the isolated case, these transition states are very similar to the physisorbed GEM form because of the presence of a triple-decker sandwich of one *p*-xylyl unit of Mac2 by two thiophenyl 1,3-diamide units of the rotating macrocycle, Mac1, and a T-shape phenyl−phenyl complex involving the phenyl core of the same *p*-xylyl unit with one of the two phenyl rings of Mac1. This state only differs from the reference state of Figure 10 by the release of a T-shape phenyl−phenyl complex, which explains its very low activation energy, yielding in turn extremely high rate constants, of the order of 10^9 s^{-1}, already at room temperature (Tables 3 and 4).

4. Conclusions

The present contribution represents one of the very first applications of molecular mechanics in the design of materials based on interlocked and highly versatile molecular systems: catenanes. In this study of two benzylic amide [2]catenanes, bearing isophthaloyl- or thiophenyl-1,3-diamide groups, I emphasize the intricacy of the intermolecular interactions (dispersion forces, π-stacks, phenyl−phenyl T- or H-shape complexes, hydrogen bonds, N−H···S bridges, etc.) and entropy effects that play a role in their physisorption on an ideally simple and well-characterized surface, graphite, and variously affect their structure and dynamics on such a surface.

Two drastically different types of physisorbed forms have been identified for the isophthaloyl-based catenane (**1**), which should coexist with significant percentages on graphite. A first mode (**A**) of physisorption enhances the role played by van der Waals interactions, since it implies a parallel layout of both macrocycles. Clearly, from the identified barriers and calculated rate constants, this mode is completely incompatible with circumrotational actions. The main reason is that, in this case, these complex and sterically demanding motions would require significant detachments of one of the interlocked macrocycles, and thus very important releases of the dispersion forces linking the catenane to graphite. A second possible mode (**B**) for physisorption of catenane **1** is the result of a competition between the dispersion interactions with the substrate on one hand and entropy effects and inter-ring interactions on the other hand. In this mode, one of the macrocycles (Mac1) remains parallel to the substrate, whereas the other one (Mac2) potrudes perpendicularly from the graphite surface. This co-conformation should allow, at least, a partial circumrotation of Mac1 about Mac2 with significant rates, as the latter has freedom enough to accommodate the high steric and electrostatic requirements of this process.

Results obtained with the thiophenyl-based catenane (**2**) indicate that enlarging the macrocyclic cavities does not necessarily suffice to ensure decent circumrotational rates on surfaces. This catenane is already enthalpically driven to a deposition mode resembling the **B**-type form of catenane **1** on graphite, which also favors π-stackings and phenyl−phenyl herringbone complexes within catenane **2** at the expense of dispersion interactions with the substrate. However, the thiophenyl rings seem to be strongly excluded from macrocyclic cavities by packing effects, strong internal electrostatic interactions, and physisorption forces. Although sterically allowed, a full circumrotational process on graphite in this catenane is thus strongly hindered at the level of, at least, the thiophenyl station. For this compound, transition state theory indicates that rates of the order of 1 macrocyclic ring rotation per second could nonetheless be reached at moderate temperatures (∼400 K).

Despite these rather deceptively too low frequencies and the limitations and artifacts of the modeling, in particular the edge effects and the too high flexibility of finite and isolated graphite layers, this study gives rise to the hope that a more favorable balance of steric, electrostatic, dispersion forces, and entropy effects in catenanes with slightly larger macrocyclic cavities would ensure ring rotations on graphite surfaces with more interesting rates at room temperature. This, together with their large freedom for translational and rotational motions on such surfaces, would open the way to the making of practical nanoscale devices with interlocked molecules.

Acknowledgment. M.S.D. is grateful to the Fonds voor Wetenschappelijk Onderzoek-Vlaanderen, the Flemish Science Foundation (Belgium), for financial support and his position as Research Leader ("Onderzoeksleider") at the Limburgs Universitair Centrum. He gratefully acknowledges Dr. F. Zerbetto (Università degli Studi di Bologna, Italy) for useful discussions and computational support. He is very grateful to Prof. J.-P. François for his kind help and careful reading. Most of the calculations reported here have been performed on a DEC 1200 station (533 MHz CPU, 2 Gby core memory, 40 Gby scratch disk) at the Limburgs Universitair Centrum.

JA992458A